

CrossMark  
click for updates

Cite this: DOI: 10.1039/c4cy01622j

Received 6th December 2014,  
Accepted 10th February 2015

DOI: 10.1039/c4cy01622j

www.rsc.org/catalysis

# Copper oxide as efficient catalyst for oxidative dehydrogenation of alcohols with air†

Raju Poreddy,<sup>a</sup> Christian Engelbrekt<sup>b</sup> and Anders Riisager<sup>\*a</sup>

The oxidative dehydrogenation of alcohols to carbonyl compounds was studied using CuO nanoparticle catalysts prepared by solution synthesis in buffered media. CuO nanoparticles synthesized in *N*-cyclohexyl-3-aminopropanesulfonic acid buffer showed high catalytic activity for the oxidation of benzylic, alicyclic and unsaturated alcohols to their corresponding carbonyl compounds with excellent selectivities. The observed trend in activity for conversion of substituted alcohols suggested a  $\beta$ -H elimination step to be involved, thus enabling a possible reaction mechanism for oxidative dehydrogenation of benzyl alcohols to be proposed. The use of CuO as an inexpensive and efficient heterogeneous catalyst under aerobic conditions provides a new noble metal-free and green reaction protocol for carbonyl compound synthesis.

## 1. Introduction

The oxidative dehydrogenation of primary and secondary alcohols to their corresponding carbonyl compounds is a fundamental reaction in nature and synthetic organic chemistry. Synthetic chemistry relies heavily on stoichiometric quantities of inorganic oxidants,<sup>1</sup> whereas nature uses metal catalysis and oxygen as the terminal oxidant.<sup>2</sup> Notably palladium,<sup>3</sup> chromium(vi) reagents<sup>4,5</sup> and manganese or ruthenium salts<sup>6,7</sup> have attracted much attention as stoichiometric oxidants. However, the application of one or more equivalents of such relatively expensive and rather toxic oxidizing agents is an important factor limiting their usage in industry today. In addition, problems relating to corrosion and plating on reactor walls, handling, recovery and reuse of the catalyst represent serious process limitations.<sup>8</sup> Therefore, the desire to replace stoichiometric oxidants with methodologies more resembling nature has gained much interest.

In the last few years numerous methods for oxidation of alcohols using heterogeneous catalysts have emerged, especially metal nanoparticles.<sup>9–11</sup> Their use of either molecular oxygen or oxygen donating agents like hydrogen peroxide as the ultimate stoichiometric oxidant makes these methods attractive and eco-friendly. In particular, molecular oxygen – or even air – has been used as a cheap and abundant oxygen

source for the oxidation of alcohols to carbonyl compounds.<sup>10</sup> Although remarkable advances have been made in heterogeneous catalysis for the selective oxidation of alcohols, particularly with transition metals, only a limited number of catalysts are effective under mild reaction conditions. Heterogeneous catalytic systems are kinetically constrained by surface availability and metal-support interactions.<sup>12</sup> Therefore, most research on aerobic oxidations using heterogeneous catalysts has focused mainly on highly active noble metals such as platinum, palladium and gold.<sup>13</sup> Despite a handful of reports on platinum and palladium as potential metals to catalyze oxidative dehydrogenation of alcohols, an overshadowing focus has emerged on gold chemistry since the pioneering work by Bond *et al.*,<sup>14</sup> Hutchings,<sup>15</sup> Haruta *et al.*<sup>16</sup> and Prati and Rossi<sup>17</sup> utilizing supported gold nanoparticles. This abrupt interest is not only because gold is cheaper than its noble metal counterparts, but also that it circumvents most of the drawbacks associated with Pt and Pd. One example is the fast deactivation rates attributed to aggregation of particles or leaching of noble metals during the oxidation and/or catalyst regeneration processes.<sup>18,19</sup> This essentially holds true for the liquid-phase oxidation of alcohols under aerobic conditions. Apart from cost considerations, the residues of noble metals (*e.g.* Pt and Pd) in pharmaceutical and nutritional products are prone to be highly harmful and problematic.<sup>20,21</sup>

Wang *et al.*<sup>22</sup> recently studied the activity of copper oxide supported gold nanoparticles and the influence of synthesis parameters on the transformation of alcohols to carbonyl compounds *via* oxidative dehydrogenation. They demonstrated that the catalytic performance of gold strongly depended on the preparation method, pH value and stirring rate by presumably influencing the electronic state and

<sup>a</sup> Centre for Catalysis and Sustainable Chemistry, Department of Chemistry, Technical University of Denmark, Kemitorvet, Building 207, DK-2800 Kgs. Lyngby, Denmark. E-mail: ar@kemi.dtu.dk; Tel: +45 45252233

<sup>b</sup> NanoChemistry, Department of Chemistry, Technical University of Denmark, Kemitorvet, Building 207, DK-2800 Kgs. Lyngby, Denmark

† Electronic supplementary information (ESI) available: Supplementary data are supplied in the Supporting Information. See DOI: 10.1039/c4cy01622j

particle size of the gold nanoparticles as well as the structure of the support. With this system there was no need for additional base to promote the reaction, which is otherwise often the case. This is good in terms of waste minimization and product recovery, but higher loading of the rather expensive noble metal gold was required to obtain moderate conversion. Hence, more sustainable solutions based on earth abundant, cheap, harmless and stable metals to replace noble metals would be desirable. In this connection, application of catalysts based on the relatively inexpensive metals Ag, Cu and Fe has increasingly been explored for aerobic and non-aerobic oxidations under ambient conditions.<sup>23</sup> Thus, silver nanoparticles or clusters supported on different metal oxides have been reported to be potential catalysts for the oxidative dehydrogenation of alcohols to carbonyl compounds.<sup>10,24</sup> Likewise, copper<sup>25,26</sup> and iron<sup>27,28</sup> have gained importance in recent years and iron oxides – although harmless, less toxic, and cheaper – are not better catalysts than copper for oxidation reactions of alcohols at low temperatures.<sup>29</sup> Other homogeneous copper catalysts<sup>30</sup> and metallic copper catalysts with styrene as the hydrogen acceptor<sup>31</sup> are also reported for alcohol dehydrogenations.

As mentioned above, Wang *et al.*<sup>22</sup> have showed that CuO is an effective support material for Au in the catalytic oxidation of alcohols. However, they also reported that CuO alone cannot catalyze the reaction being nearly inactive, since the adsorption of benzyl alcohol onto the CuO surface was too weak to be activating and that pure CuO could not activate the O<sub>2</sub> molecule. Copper, because of its characteristic promoting ability, was also involved in bi-metallic catalysis particularly with gold<sup>32</sup> and platinum.<sup>33</sup> Our interest in the synthesis of carbonyl compounds as well as non-noble metal catalysis prompted us to examine a range of supported copper-based catalysts for alcohol oxidation.

In this work, we have elaborated our previous synthesis procedure for CuO nanoparticles and the structure and morphology of the CuO catalysts have been thoroughly characterized. We further demonstrate that CuO as a non-noble metal oxide is a highly efficient heterogeneous catalyst in the oxidation of alcohols under mild reaction conditions using oxygen as a green terminal oxidant.

## 2. Experimental section

### 2.1 Chemicals

CuCl<sub>2</sub>·2H<sub>2</sub>O (*p.a.*, Riedel-de Haën), *N*-cyclohexyl-3-aminopropanesulfonic acid (CAPS) (≥98%, Sigma-Aldrich), 2-(*N*-morpholino)ethanesulfonic acid (MES) hydrate (99.5%, Sigma-Aldrich), and KOH (≥85%, Sigma-Aldrich) were used as received for the synthesis of CuO nanoparticles. All the substrates for the catalytic oxidations were purchased from Sigma Aldrich and used without any further purification.

### 2.2 Catalyst preparation

CuO nanoparticles were synthesized following a modification of our previously reported procedure.<sup>34</sup> It was found that pH

about 11 is optimal for aqueous CuO synthesis. Therefore, CAPS (pK<sub>a</sub> = 10.4) was chosen to replace MES (pK<sub>a</sub> = 6.15) as the buffer. Preparation was done by first dissolving 4.432 g of CAPS (nanoparticles denoted “CAPS-CuO”) or 3.905 g of MES (nanoparticles denoted “MES-CuO”) in 950 mL of Millipore water and adjusting the pH to 11 for CAPS-CuO and 12 for MES-CuO with KOH. The buffer was preheated to 95 °C under stirring before rapid addition of a 50 mL solution of 0.682 g of CuCl<sub>2</sub> in Millipore water. Final concentrations of buffer and CuCl<sub>2</sub> were 20 and 4 mM, respectively. The initially bright blue CuCl<sub>2</sub> solution immediately turned green indicating intermediate formation of hydrated copper hydroxide and after few seconds the solution turned dark brown as CuO was formed. Heating was maintained for 30 min after which the solution was allowed to cool to room temperature with stirring. Stirring was terminated and the particles were left to sediment overnight. The CuO nanoparticles were filtered under vacuum with a 0.2 μm Nylon membrane filter from Gelman Sciences (New York, USA) and washed several times with water. The remaining water was expelled from the product by washing with ethanol, and then dried under vacuum to remove excess ethanol leaving a brittle film that could easily be recovered from the membrane. The dry powder was lightly crushed and left under vacuum overnight.

Two different samples of Cu<sub>2</sub>(OH)<sub>3</sub>Cl were tested as reference systems. A-Cu<sub>2</sub>(OH)<sub>3</sub>Cl was prepared in a similar procedure to the CuO nanoparticles but in 1.5 L batches and final concentrations of MES and CuCl<sub>2</sub> of 50 and 10 mM, respectively. The buffer was adjusted to pH 11 and preheated to 80 °C before CuCl<sub>2</sub> addition. The synthesis of B-Cu<sub>2</sub>(OH)<sub>3</sub>Cl was achieved by heating a mixture of Cu<sub>2</sub>(OH)<sub>2</sub>CO<sub>3</sub> and CuCl<sub>2</sub> as described previously.<sup>32</sup>

### 2.3 Catalyst characterization

The textural properties of the samples were determined by nitrogen physisorption analysis using a Micromeritics (Norcross, GA, USA) ASAP 2020 with an Automated Gas Adsorption Surface area and Porosimetry Analyzer at liquid nitrogen temperature. The samples were outgassed in vacuum at 200 °C prior to measurement. The surface areas were determined by the Brunauer–Emmett–Teller (BET) method.

X-ray powder diffraction (XRD) spectra were measured on a Huber (Rimsting, Germany) G670 diffractometer with a Guinier imaging plate camera operated in transmission mode with CuKα<sub>1</sub> (λ = 1.54 Å) irradiation from a focusing quartz monochromator. The samples were fixed between two pieces of Scotch tape and rotated during data collection. The diffraction patterns of the samples were recorded at room temperature in the 2θ range of 3–100° in steps of 0.005°.

Transmission electron microscopy (TEM) studies were performed using a Tecnai T20 G2 and Titan instrument from FEI Company (Hillsboro, OR, USA) operated at 200 and 120 kV, respectively. The Titan was fitted with a field-emission electron source and a spherical aberration corrector on the condenser lens system. The samples were redispersed in

ethanol by ultrasonication and deposited on plain or holey carbon-coated Cu grids from Agar Scientific (Stansted, UK).

X-ray photoelectron spectroscopy (XPS) was performed with a Thermo Scientific XPS using Al-K $\alpha$  (1486 eV) as the excitation X-ray source. The pressure of the analysis chamber was maintained at  $2 \times 10^{-10}$  mbar during measurement. The XPS measurements were performed in the electron binding energy ranges corresponding to copper 2p and oxygen 1s core excitations.

The reducibility of the copper catalysts was investigated by temperature programmed reduction using H<sub>2</sub> (H<sub>2</sub>-TPR). The samples were pretreated in 20 mL min<sup>-1</sup> 10% O<sub>2</sub>-He mixture gas flow at 500 °C for 1 h and then cooled down to 30 °C and flushed out with He for 1 h. Then the samples were heated from 30 to 600 °C at a ramp of 10 °C min<sup>-1</sup> in 60 mL min<sup>-1</sup> 4% H<sub>2</sub>-Ar mixture gas flow. The water formed during reduction with H<sub>2</sub> was trapped using a dry ice cold trap and the hydrogen consumption was continuously monitored with a TCD detector.

The amount of copper leached into the reaction liquor after the catalytic reactions was determined by inductively coupled plasma mass spectrometry (ICP-MS). Toluene was removed from 1 mL of filtrate after 24 h reaction by drying and the remnant, containing any leached copper, was dissolved in 5 mL of 0.1 M nitric acid for analysis. 4 mg of fresh com-CuO was similarly dissolved in 5 mL of 0.1 M nitric acid.

Thermogravimetric analysis of catalysts was performed using a TGA/DSC 1 STAR system from Mettler Toledo in 80 mL min<sup>-1</sup> N<sub>2</sub> flow and a heating rate of 10 °C min<sup>-1</sup>.

Attenuated total reflectance Fourier transform infrared spectroscopy (ATR-FTIR) measurements were performed using a Thermo Scientific Nicolet iS5 and Specac Golden Gate (Waltham, MA, USA) with a diamond plate. The spectra were recorded in the range of 4000–400 cm<sup>-1</sup> with a resolution of 2 cm<sup>-1</sup>.

## 2.4 General oxidation procedure

In a typical oxidation reaction, the copper catalyst (60 mg, 0.75 mmol, 75 mol% with respect to the substrate) was dispersed in a glass tube in 3 mL of toluene facilitated by ultrasonication followed by the addition of substrate (1 mmol) and internal standard anisole (0.1 mmol). The tube containing the reaction mixture was connected to a reaction station which provided stirring and heating at 100 °C for 22–24 h. The reaction was carried out under atmospheric pressure of air with oxygen as the oxidant.

## 2.5 Product analysis

During the reactions samples were periodically collected, filtered and analyzed by GC-FID (Agilent, 6890N) and GC-MS (Agilent, 6850N) with an HP-5 capillary column (Agilent, J&W) using N<sub>2</sub> as the carrier gas. The amounts of substrates and reaction products were quantified using anisole as an

internal standard. The reported conversions were calculated from the conversion of alcohol.

# 3. Results and discussion

## 3.1 Catalyst preparation

In our previous work, copper mineral nanoparticles (CuO and Cu<sub>2</sub>(OH)<sub>3</sub>Cl) were selectively synthesized by controlling pH with a buffered reaction medium. The optimal conditions for CuO formation were determined to be 95 °C and pH 11. For the current work, the synthesis was further optimized for the preparation of the CuO catalysts. A Good's buffer with a pK<sub>a</sub> close to pH 11 was chosen (CAPS, pK<sub>a</sub> = 10.4) and the reactant concentrations increased providing well-defined CuO nanoparticles in less than 30 min.

## 3.2 Catalyst screening

The oxidation of benzyl alcohol was investigated in the presence of a range of commercial and synthesized copper catalysts in toluene at 100 °C and atmospheric pressure of air. The reaction proceeded smoothly to afford the corresponding aldehydes with good to excellent yields. Table 1 compiles the catalytic performance obtained with Cu(I) and Cu(II) oxides, chlorides and hydroxychlorides (Table 1, entries 1–10) for aldehyde formation under the given reaction conditions.

The CuO synthesized in different buffered media (*i.e.* CAPS-CuO and MES-CuO) showed activity and selectivity superior to other tested catalysts for benzaldehyde formation (Table 1, entries 1 and 2). Hence, MES-CuO with an excellent selectivity of >99% yielded 71% benzaldehyde whereas CAPS-CuO afforded >99% yield of benzaldehyde. Over-oxidation or aldehyde disproportionation products such as acids, esters, and alcohols were not observed during the reaction.

The commercial copper oxide nanopowder (com-CuO) with a particle size of <50 nm and a surface area of 13.1 m<sup>2</sup> g<sup>-1</sup> (Table 1, entry 3) performed best of the commercial catalysts (entries 7–10). The lack of significant activity of the bulk CuO (entry 7) may be ascribed to the low BET surface

**Table 1** Catalyst screening for aerobic oxidation of benzyl alcohol<sup>a</sup>

Entry	Catalyst	S <sub>BET</sub> [m <sup>2</sup> g <sup>-1</sup> ]	Conversion <sup>b</sup> [%]	Selectivity [%]
1	CAPS-CuO	46.2	>99	>99
2	MES-CuO	37.4	71	>99
3	com-CuO	13.1	69	91
4	com-CuO <sup>c</sup>	n.d. <sup>d</sup>	4	>99
5	A-Cu <sub>2</sub> (OH) <sub>3</sub> Cl	20.1	23	>99
6	B-Cu <sub>2</sub> (OH) <sub>3</sub> Cl	5.1	29	>99
7	CuO bulk	n.d. <sup>d</sup>	3	>99
8	Cu <sub>2</sub> O bulk	0.10	2	>99
9	CuCl	n.d. <sup>d</sup>	5	>99
10	CuCl <sub>2</sub>	5.3	16.7	89
11 <sup>e</sup>	—	—	2	>99

<sup>a</sup> Reaction conditions: benzyl alcohol (2 mmol), anisole (0.2 mmol), toluene (6 mL), 120 mg catalyst, 24 h, 100 °C, atmospheric air.

<sup>b</sup> Conversion was evaluated by GC and GC-MS using anisole as internal standard. <sup>c</sup> Reduced com-CuO using H<sub>2</sub> (10% in N<sub>2</sub>). <sup>d</sup> Not detectable. <sup>e</sup> Control experiment without catalyst.

area. Although com-CuO was more active than the other commercial catalysts, it was less selective. Thus, over-oxidation of benzaldehyde to benzoic acid followed by esterification seemed unavoidable with com-CuO resulting in lower selectivity (91%) than CAPS- and MES-CuO.

The formation of the over-oxidation product benzyl benzoate can also be obtained by oxidation of the hemiacetal (a product resulting from the reaction of benzyl alcohol and benzaldehyde). Copper(II) chloride (entry 10) showed some activity for benzaldehyde formation, but catalysed also the nucleophilic exchange reaction with benzyl alcohol yielding benzyl chloride and alkylation of toluene (solvent) with benzyl alcohol in significant amounts. The catalysis of side reactions was not observed for the synthesized hydroxychlorides (entries 5 and 6). Their activity was improved compared to  $\text{CuCl}_2$  but still not comparable to the synthesized oxides. com-CuO was reduced at 300 °C by  $\text{H}_2$  (10% in  $\text{N}_2$ ) to its metallic state and studied for the same reaction (entry 4). The reduction of com-CuO did not improve the activity but instead reduced it to only 4%. In fact, only copper in the oxidation state +2 showed any significant activity for the oxidation of benzyl alcohol. A control experiment without added catalyst was further performed and, as expected, no substantial amount of benzaldehyde was formed under the given reaction conditions (entry 11).

### 3.3 Characterization of CAPS-, MES- and com-CuO

Detailed characterization of the catalysts (especially CAPS-CuO which exhibited superior performance) was undertaken to correlate their activity and structural properties. The crystal structure and morphology of the synthesized nanostructures were characterized by XRD and TEM. Fig. 1a and c

displays the fitted XRD patterns of CAPS-CuO and MES-CuO, respectively. Both catalysts showed clear tenorite CuO structure and no other detectable crystalline phases. This is supported by Rietveld refinement of the spectra confirming previous findings that no redox process was involved in the synthesis.<sup>32</sup> The refinement provided crystallite sizes of 17.5 and 18.8 nm for CAPS-CuO and MES-CuO, respectively. Apart from the small variation in crystallite size, no differences were detected with XRD. The purity of the as-synthesized CAPS-CuO was further confirmed by ICP-MS measurements of the dissolved catalyst showing no other metal impurities (ESI† Fig. S1).

The morphology, *i.e.* shape, size and roughness, of the CuO nanoparticles was investigated with TEM which is supplementary to the crystallite information from XRD. High and low magnification TEM micrographs of CAPS- and MES-CuO are presented in Fig. 2. Both catalysts consist of flat, elongated nanoparticles up to 200 nm long, 100 nm wide and roughly 10 nm thick (Fig. 2a and e). The particles are seemingly assembled by rods *via* side-to-side attachment and overall smaller in CAPS-CuO than MES-CuO. The rod-like structures and rough surfaces are evident in Fig. 2b and f. Due to the aggregating nature of the nanoparticles on the TEM grids it was difficult to obtain electron diffraction from single particles. Instead, the nanoscale crystal structure was studied by high-resolution (HR) TEM. HR micrographs of several single nanoparticles from CAPS- and MES-CuO were obtained and the corresponding FFTs indexed (Fig. 3 and ESI† Table S1).

The facets making up the main surface of the crystals were determined from the zone axis with the assumption that the flat structures were lying roughly perpendicular to the beam. The crystal directions corresponding to the long, intermediate and short axes of the sheets were identified as [010], [100]

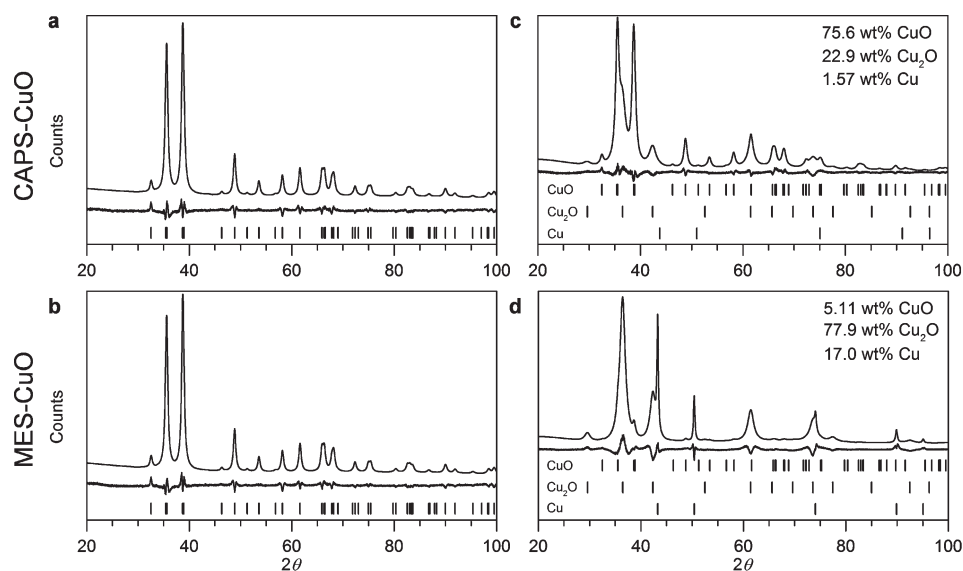


**Fig. 1** Rietveld refinements of fresh (a) CAPS-CuO and (b) MES-CuO catalysts and the corresponding profiles for spent (c) CAPS-CuO and (d) MES-CuO after 22 h of oxidation of benzyl alcohol in toluene at 100 °C in air. Each graph includes the refined pattern (top line), the difference between the refinement and raw data (bottom line) and Bragg positions of crystallographic phases of CuO,  $\text{Cu}_2\text{O}$  and metallic copper (black bars).



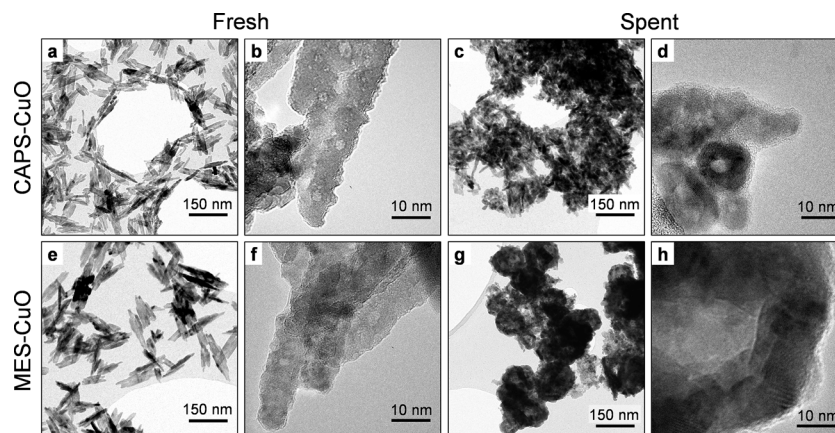


**Fig. 2** TEM micrographs of the as-synthesized (a–b) CAPS-CuO and (e–f) MES-CuO, and the corresponding spent (c–d) CAPS-CuO and (g–h) MES-CuO after 24 h of benzyl alcohol conversion at 100 °C in air. TEM images of as-received com-CuO are shown in the ESI† Fig. S2.

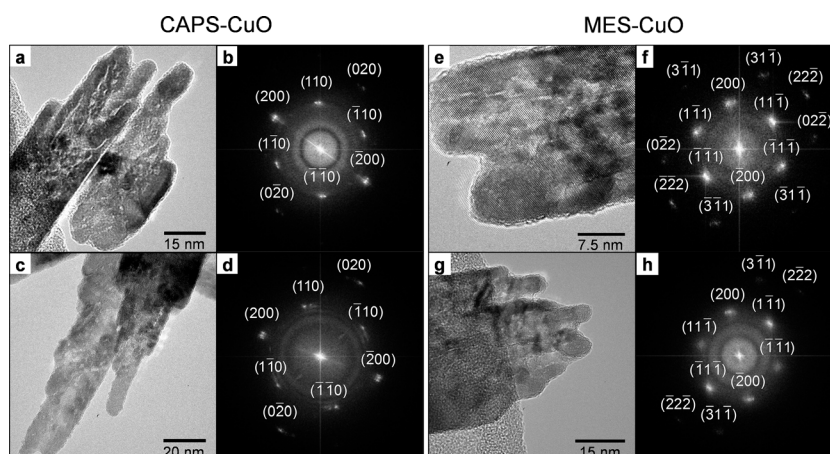


**Fig. 3** Representative HR-TEM micrographs of (a, c) CAPS- and (e, g) MES-CuO with corresponding indexed FFTs for (b, d) CAPS-CuO and (f, h) MES-CuO.

and [001] for CAPS-CuO and [01-1], [100] and [011] for MES-CuO, respectively. These observations indicate that while the overall crystallite size and nanoparticle shape were similar for the two structures the different chemical environments during synthesis may have led to changes in the relative surface energies of the main facets and oriented attachment mechanisms. The slight differences in exposed facets may contribute to the differences in observed activity (Table 1) as the main facets may represent different inherent activities towards the dehydrogenation of benzyl alcohol. Similar anisotropic growth and [OH<sup>-</sup>] dependency have previously been observed.<sup>35–38</sup>

Fig. 4 shows the XPS spectra corresponding to the Cu 2p transition for CAPS- and com-CuO. The peaks at binding energies of about 934.2 and 953.0 eV (full spectrum, ESI† Fig. S3) are due to the spin-orbit doublet of the Cu 2p core level transition. The Cu 2p<sup>3/2</sup> transition included in Fig. 4 of both CAPS- and com-CuO can be deconvoluted giving two main contributions located around 934.2 and 937.5 eV. The relatively sharp band located at 934.2 eV is tentatively assigned to CuO,<sup>39</sup> while the second peak located at 937.5 eV

is allocated to Cu(II) species with different environment or coordination.<sup>40</sup> Full range spectra of both CAPS- and com-CuO are shown in the ESI† Fig. S3 with spin-orbit coupled Cu 2p<sup>1/2</sup> transition (953.0 eV) between two well defined satellite structures at around 945.1 and 956 eV.

McIntyre *et al.*<sup>41</sup> have reported that the main Cu 2p<sup>3/2</sup> transition for metallic copper and Cu<sub>2</sub>O appears at energy levels lower than 933 eV, while it shifts to values higher than 933 eV for Cu(II) species. The Cu 2p<sup>3/2</sup> transition for Cu(0) and Cu(I) was reported to occur at the same binding energy of 932.5 eV, about 1.3 eV below the main core level line.<sup>39,42</sup> According to this assignment, the profiles shown in Fig. 4 reveal neither Cu(0) nor Cu(I) in synthesized and commercial copper oxide. A satellite peak located above the core level line (945.1 eV) is prominent in both CuO samples (ESI† Fig. S3), but hardly visible in Cu(I) XPS.<sup>40</sup> This observation confirms that the oxidation state of Cu in both catalysts is +2 and is consistent with the XRD results. However, the energy of the Cu 2p<sup>3/2</sup> transition does not allow unequivocally determination of the oxidation state of copper unless the Auger parameter ( $\alpha$ ) is determined.<sup>38</sup> Furthermore, a relatively narrow line

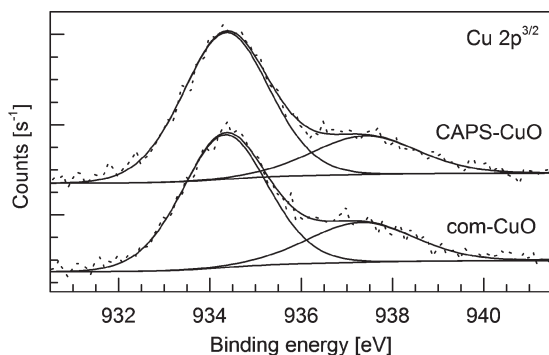


Fig. 4 High resolution XPS core level spectra of the Cu 2p transition for CAPS-CuO (top) and com-CuO (bottom).

(FWHM = 1.8 eV) at around 532.5 eV representing O 1s<sup>1/2</sup> transition was observed for both of the catalysts<sup>41</sup> (ESI† Fig. S4). This transition appears to arise mainly from one type of oxygen. It has been reported that the CuO phase likely has three types of oxygen components, namely O–Cu, HO–Cu, and surface oxygen (O-surf) with binding energies around 529.1, 530.6, and 531.5 eV, respectively.<sup>43</sup> This clearly suggests that both catalysts (CAPS- and com-CuO) have a high degree of surface oxygen.

Additional information about the copper species in the CAPS- and com-CuO catalysts was obtained by H<sub>2</sub>-TPR (Fig. 5). The H<sub>2</sub> consumption was also studied for bulk CuO and Cu<sub>2</sub>O to elucidate how bulk copper species behave differently from highly dispersed surface Cu species on CAPS- and com-CuO. Interestingly, the reduction temperatures for CAPS- and com-CuO were very low compared with those of bulk CuO and Cu<sub>2</sub>O, suggesting that bulk species were reduced at higher temperatures than Cu(II) on the surface. The low temperature peaks of TPR due to highly dispersed CuO and/or Cu(II) species have also been observed for supported CuO.<sup>44,45</sup> Van der Grift *et al.*<sup>46</sup> and Robertson *et al.*<sup>47</sup> further supported this observation concluding that the highly dispersed copper oxide species are more easily reduced than bulk CuO. CAPS-CuO seemed to have no bulk copper oxide and was therefore reduced at very low temperatures, while com-CuO comprises both dispersed and bulk-like CuO

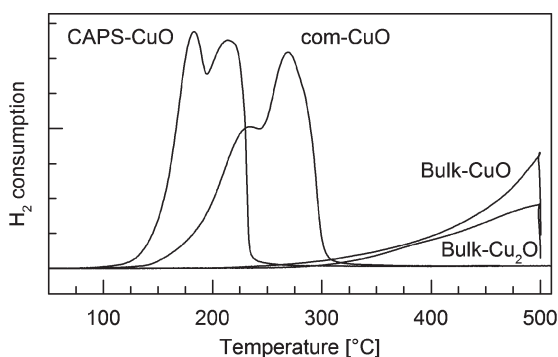


Fig. 5 H<sub>2</sub>-TPR profiles of different copper catalysts.

resulting in a shift in reduction peak to higher temperatures without exhibiting true bulk behavior. At this point, it is worth noting that the specific surface area of highly dispersed CAPS-CuO (46.2 m<sup>2</sup> g<sup>−1</sup>) was substantially higher than that of com-CuO (13.1 m<sup>2</sup> g<sup>−1</sup>). Hence, more active Cu(II) species were available providing increased catalytic activity.

### 3.4 Optimization of reaction conditions

CAPS-CuO as the best performing catalyst was used to optimize the reaction conditions. In order to investigate the effect of the atmosphere, the reaction was tested under air, argon, pure oxygen and wet oxygen conditions (Fig. 6).

Reaction in atmospheric air resulted in higher yields (>99%) than inert (10%), pure oxygen (21%) and wet oxygen (28%) conditions. These results underlined that oxygen was essential for the reaction, but also suggested that only a moderate amount of oxygen was beneficial for the reaction. Increased oxygen concentration could lead to saturation of the surface by oxygen. As a result, the rate of aldehyde formation could be lowered. Furthermore, the wet oxygen experiment confirmed the activity to increase by almost 50% compared to dry oxygen conditions. XRD results of the four spent catalysts revealed an interesting observation that copper oxide was partially reduced only in air, while no reduction apparently occurred under the conditions where only low or insignificant conversions were obtained (ESI† Fig. S5a).

The catalytic activity of the prepared CAPS-CuO was tested using atmospheric air at different temperatures to further optimize the reaction conditions. As shown in Table 2, the conversion of benzyl alcohol to benzaldehyde after 24 h increased from 11 to >99% when the temperature was increased from 40 to 100 °C. The catalyst was observed to be more selective for benzaldehyde at higher temperatures with a change in selectivity from 95 to 99% in 24 h.

The effect of catalyst loading was further studied with CAPS-CuO at 100 °C in air with catalyst mass between 10 and 60 mg (Fig. 7). Not surprisingly, the overall reaction rate was found to increase with the amount of catalyst and even 20 mg (25 mol%) of the catalyst gave 75% yield in 24 h.

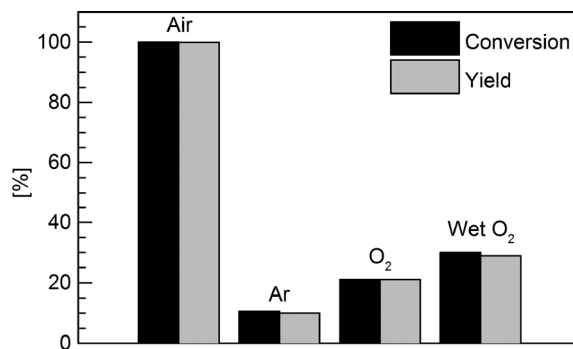
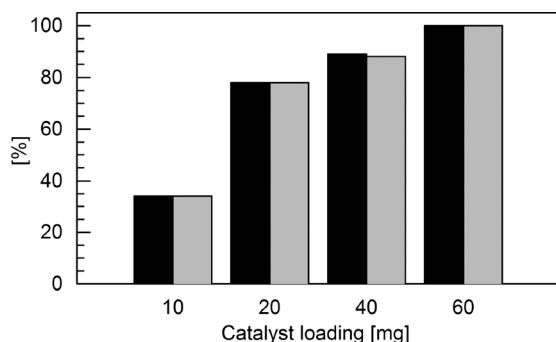


Fig. 6 Effect of atmosphere on benzyl alcohol oxidation. Reaction conditions: benzyl alcohol (1 mmol), anisole (0.1 mmol), toluene (3 mL), 60 mg CAPS-CuO catalyst, 24 h, 100 °C.

**Table 2** Influence of temperature on the activity of catalyst CAPS-CuO<sup>a</sup>

Entry	Temp. [°C]	Conversion <sup>b</sup> [%]	Selectivity <sup>b</sup> [%]	Yield <sup>b</sup> [%]
1	40	11 (5)	95 (>99)	10 (5)
2	60	21 (9)	97 (99)	20 (9)
3	80	49 (18)	98 (98)	48 (18)
4	100	>99 (36)	>99 (97)	>99 (35)

<sup>a</sup> Reaction conditions: benzyl alcohol (1 mmol), anisole (0.1 mmol), toluene (3 mL), 60 mg catalyst, 24 h, atmospheric oxygen. <sup>b</sup> After 24 h and after 6 h in parentheses.



**Fig. 7** Effect of CAPS-CuO catalyst loading on oxidation of benzyl alcohol showing conversion (black) and yield (grey). Reaction conditions: benzyl alcohol (1 mmol), anisole (0.1 mmol), toluene (3 mL), 24 h, 100 °C, atmospheric air.

Furthermore, the selectivity of the reactions seemed independent of the catalyst loading with only insignificant amounts (1%) of esterification product (benzyl benzoate) observed for the reaction run with 40 mg of catalyst. In terms of reaction time, conversion and selectivity a loading of 60 mg of CAPS-CuO catalyst was considered optimal and thus maintained for further experiments. This corresponds to 75 mol% and approaches stoichiometric amounts. However, this is less important since it is a non-precious metal and can be successfully regenerated (see section 3.8).

Fig. 8 shows the time-dependent catalytic performance of commercial CuO (com-CuO) in comparison with the prepared CuO (CAPS- and MES-CuO). The initial reaction rate was low and similar for the three CuO catalysts, indicating that an induction period prevailed before reaching full activity. Thus, after 4 h of reaction the conversion of benzyl alcohol had reached only about 11% for all of the catalysts. However, at prolonged reaction time of 24 h the CAPS-CuO provided >99% yield of benzaldehyde, whereas the reaction rate was lower for the MES- and com-CuO yielding only 69 and 70% benzaldehyde in 24 h, respectively. The origin of the induction period could be related to low initial surface–substrate interaction, heating of the solvent from room temperature to the target temperature, or catalyst wetting processes although this is not presently disclosed.

The stability of the catalysts can be closely related to the ability to maintain a high amount of Cu(II) avoiding transformation into Cu(I) and especially metallic Cu, both of which have shown poor activity. The phase transition in CAPS- and

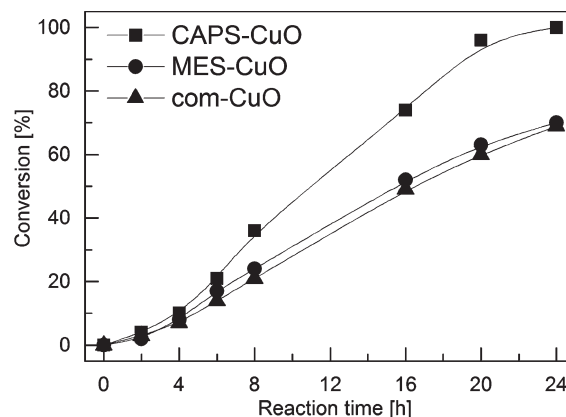


**Fig. 8** Conversion of benzyl alcohol with time over CAPS-CuO, MES-CuO, and com-CuO (commercial) catalysts. Reaction conditions: benzyl alcohol (1 mmol), anisole (0.1 mmol), toluene (3 mL), catalyst (60 mg) 24 h, 100 °C, atmospheric air.

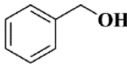
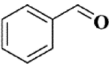
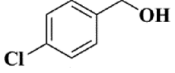
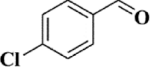
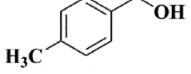
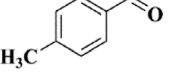
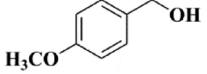
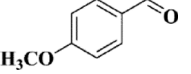
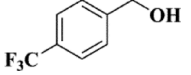
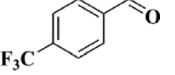
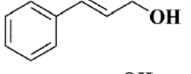
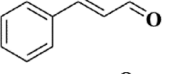
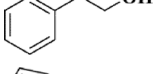
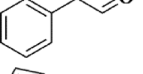
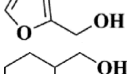
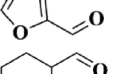
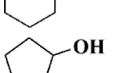
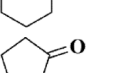
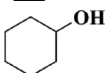
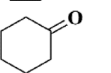
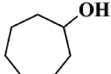
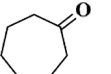
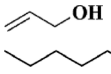
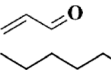
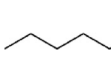
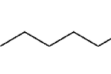
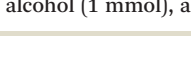
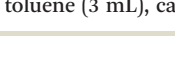
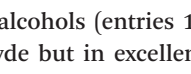

MES-CuO and the distribution of CuO, Cu<sub>2</sub>O and Cu metal were monitored by XRD of the catalysts after 24 h of reaction (Fig. 1b and d). Catalyst CAPS-CuO was reduced partially with time (ESI† Fig. S5b) to Cu<sub>2</sub>O, but not to an extent that could affect the reaction rate. The reduction was more pronounced in the case of the MES-CuO catalyst, where only about 5 wt% of the copper remained as CuO.

The partial reduction of the CuO nanoparticles led to a change in morphology. The spent MES-CuO catalyst showed a large number of spherical, hollow structures around 100 nm in size (Fig. 2g). These were not present in the spent CAPS-CuO sample where only a few 10 nm spherical structures were found. It is clear that the slight difference in the synthesis procedure of the two copper oxides had great influence on the stability resulting in the superior performance of CAPS-CuO. This agrees with the HR-TEM results showing that the surface of CAPS-CuO is dominated by highly stable [001] facets.<sup>34,35</sup> com-CuO resulted most likely in lower catalytic activity than the CAPS-CuO catalyst, because of its substantially lower surface area and the absence of well-defined crystallinity (ESI† Fig. S2).

### 3.5 Versatility of the reaction

With the optimized reaction conditions established, the scope of aldehyde and/or ketone formation was examined with the CAPS-CuO catalyst. The substrates were carefully chosen to demonstrate the versatility of the reaction between saturated and unsaturated alcohols, aromatic and alicyclic alcohols, and substituted and unsubstituted alcohols (Table 3). The results confirmed that conversion of a broad range of alcohols was achieved with excellent  $\geq 98\%$  selectivity except for cinnamyl alcohol which only gave 61% selectivity at full conversion (Table 3, entry 6) due to benzopyran formation (cyclization product). Thus, importantly the unsaturated alcohols, allyl alcohol and cinnamyl alcohol (entries 6 and 13), yielded the desired aldehydes in good to excellent yields without loss of the carbon double bonds. The

**Table 3** Catalytic oxidation of various alcohols over CAPS-CuO with air<sup>a</sup>

Entry	Substrate	Product	Conversion [%]	Selectivity [%]
1			>99	99
2			75	>99
3			98	98
4			100	98
5			61	>99
6			100	61
7			6	>99
8			98	99
9			27	>99
10			3	98
11			7	>99
12			>99	>99
13 <sup>b</sup>			>99	96
14			7	>99
15			6	>99

<sup>a</sup> Reaction conditions: alcohol (1 mmol), anisole (0.1 mmol), toluene (3 mL), catalyst (60 mg), 24 h, 100 °C, atmospheric air. <sup>b</sup> 80 °C.

saturated aliphatic alcohols (entries 14 and 15) afforded very low yields of aldehyde but in excellent selectivity, suggesting that longer reaction time (or higher temperature) than compared to benzyl alcohol was needed to reach high yields.

To study the effect of ring strain on the activity cyclopentanol, cyclohexanol and cycloheptanol (entries 10–12) were also included as substrates. Interestingly, the activity towards these alcohols increased markedly with ring size, *i.e.* the number of carbon atoms in the ring. This was most pronounced in the case of cycloheptanol where >99% yield of cycloheptanal was obtained. These results are well-matched with previously reported results by Wang *et al.*,<sup>22</sup> that tension in the ring increases with the size leaving the molecule more reactive. Furthermore, Wang *et al.* also reported that *para*-substituents had no obvious effect on the catalytic oxidation rates of benzyl alcohols with Au/CuO under the given conditions. This is understandable if benzyl carbocation

intermediates are not generated of which stability (and thus reactivity) would strongly depend on the *para* substituent. Arguably, a reaction mechanism including  $\beta$ -H elimination is still proposed in the work. In our work, different *para*-substituted benzyl alcohols were also tested as substrates in the CuO catalyzed oxidation reaction (Table 3, entries 2–5).

A significant decrease in substrate conversion was observed with the substituents in the following order: *p*-OCH<sub>3</sub> (100%) > *p*-CH<sub>3</sub> (98%) > *p*-Cl (75%) > *p*-CF<sub>3</sub> (61%). This suggests a linear free energy relationship between the activity and the Brown–Okamoto ( $\sigma^+$ ) parameter, where substrates with electron donating groups (*p*-OCH<sub>3</sub> and *p*-CH<sub>3</sub>) are more reactive than those with electron withdrawing groups (*p*-Cl and *p*-CF<sub>3</sub>). These results clearly indicate that the reaction proceeded *via* a rate determining  $\beta$ -H elimination step resulting in the formation of an intermediate benzyl carbocation. Such an elimination step is also generally found

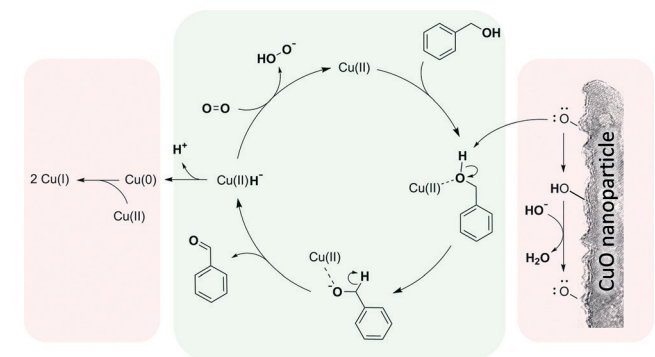


to be the rate determining step.<sup>48,49</sup> The slight decrease (1–2%) found in selectivity to benzylic aldehydes (Table 3, entries 1–5) was due to the formation of the corresponding esters. Such esters may be formed by condensation of the benzyl alcohols with benzoic acids (from over-oxidation of aldehyde or aldehyde disproportionation) or by oxidation of the hemiacetals (from reaction of benzyl alcohols with benzaldehydes).

### 3.6 Mechanism of oxidation

The XRD measurements showed that part of the CuO catalyst was reduced during reaction initially forming Cu<sub>2</sub>O and eventually metallic Cu. The amount of reduced copper increased with the reaction time (ESI† Fig. S5b). Copper was reoxidized to CuO after regeneration by calcining at 300 °C for 30 min (ESI† Fig. S6). The observation of reduced copper in experiments with high conversion and the lack of Cu(0) in reactions with low conversion (*i.e.* under an atmosphere other than air) suggests that redox cycling of active copper centers may be involved in the reaction mechanism.

A simplified mechanism for CuO catalyzed benzaldehyde formation under aerobic conditions is proposed in Scheme 1 in agreement with reports by Abad *et al.* and Frstrup *et al.*<sup>49</sup> In the cycle, benzyl alcohol adsorbs on a copper site forming a metal-alkoxide intermediate. The hydroxy proton is abstracted by a neighbouring surface oxygen. Subsequently,  $\beta$ -H elimination facilitated by Cu(II) generates Cu(II) hydride and a benzyl carbocation intermediate followed by aldehyde formation. In the final step, atmospheric oxygen reacts with the hydride forming the peroxide anion and regenerating the catalytic Cu(II) site. Reaction of the peroxide anion with a second hydride reduces it further to hydroxide anions. These hydroxide anions react in an off-cycle mechanism with the protonated surface oxygen to produce water as the only by-product. Further studies have been initiated to elucidate the mechanistic pathway. The observed reduction of the CuO may arise from deprotonation of the hydride intermediate forming Cu(0) and subsequent comproportionation of Cu(0) and adjacent Cu(II) to form Cu(I).



**Scheme 1** Simplified reaction mechanism for the CuO catalyzed oxidation of benzyl alcohol with atmospheric oxygen.

### 3.7 Reaction heterogeneity

To assess the heterogeneity of the reaction, a hot filtration test was performed after 8 and 24 h of the reaction with the CAPS-CuO catalyst (Fig. 9). After removal of the catalyst after 8 h of reaction, no further conversion was observed indicating that active species did not leach to the reaction liquor. However, after 24 h of reaction a trace amount of copper was indeed observed by ICP-MS in the reaction phase (ESI† Fig. S1). Interestingly, the leached copper species did not catalyze the reaction homogeneously when excess benzyl alcohol was added to the filtrate, and the yield remained on the same level (2–3%) as found in the blank experiment after 48 h of reaction (Table 1, entry 11). These findings clearly ruled out that leached copper species contributed to the oxidation of benzyl alcohol.

### 3.8 Reusability studies

An imperative feature of heterogeneous catalysts is their recovery from the reaction medium and reuse. The prepared CAPS-CuO catalyst could easily be separated from the reaction mixture by filtration followed by drying (120 °C, 1 h) and reused in the oxidation of benzyl alcohol as shown in Fig. 10. In the second reaction run the catalytic performance remained unchanged with conversion and yield of >99%, showing the apparent stability of the prepared catalyst. However, during further reuse the catalyst lost activity leading to a gradual decrease in conversions to 53, 7 and 2% in the successive third, fourth and fifth reaction run, respectively. Notably, the conversion after the fifth run (2%) was equal to the conversion obtained without the presence of the catalyst (Table 1, entry 11).

From the findings of TGA (ESI† Fig. S7), it was evident that the spent catalyst lost 11 wt% when treated at 250 °C in air. This suggested that carboxylate deposits had accumulated on the active sites of Cu restricting the accessibility to

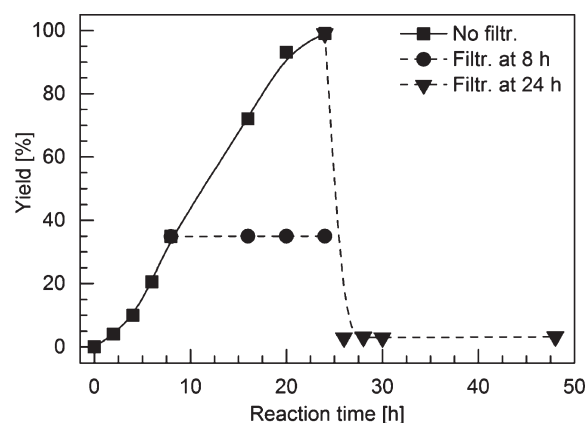


**Fig. 9** Yields from separate hot filtration experiments where the CAPS-CuO catalyst was removed by filtration and the reaction filtrate was allowed to react further. (●): Catalyst removed after 8 h. (▼): Catalyst removed after 24 h followed by addition of 1 mmol substrate and continued reaction for another 24 h. (■): Results with catalyst from Fig. 8 (for comparison). Reaction conditions: benzyl alcohol (1 mmol), anisole (0.1 mmol), toluene (3 mL), catalyst (60 mg), 100 °C, atmospheric air.

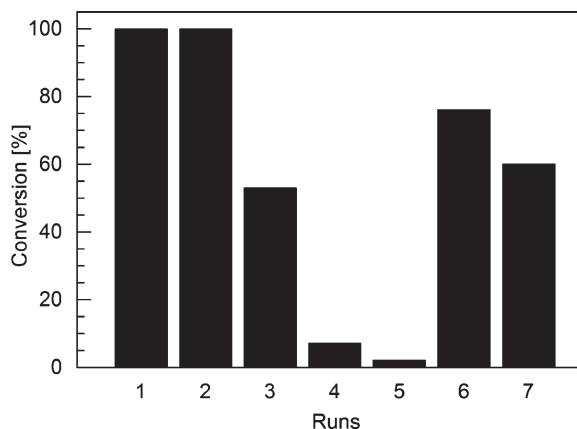


Fig. 10 Reuse of the CAPS-CuO catalyst in the oxidation of benzyl alcohol with intermediate drying at 120 °C for 1 h (until run 5). Reaction conditions: benzyl alcohol (1 mmol), anisole (0.1 mmol), toluene (3 mL), catalyst (60 mg), 24 h, 100 °C, atmospheric air.

the substrate. This was further supported by ATR-FTIR where a weak absorbance between 1300 and 1650  $\text{cm}^{-1}$  was observed (ESI† Fig. S8). Hence, if the catalyst was pre-heated at 600 °C for 30 min before being reused again in a sixth reaction run the catalyst regained a significant part of its original activity and 76% conversion was obtained (Fig. 10). However, a significant decrease in activity to about 60% conversion (99% selectivity) was again obtained after yet another reaction run (seventh run), possibly due to agglomeration of copper oxide particles facilitated by the thermal regeneration process.

Another reusability study was performed with fresh catalyst and intermediate re-activation at 300 °C for 45 min (instead of 600 °C for 30 min) (Fig. 11). As expected, the catalyst demonstrated here almost consistent performance for four consecutive catalytic runs with consistent conversion and selectivity of  $\geq 97\%$  (the slight decrease in conversion in the third run is attributed to an experimental error).

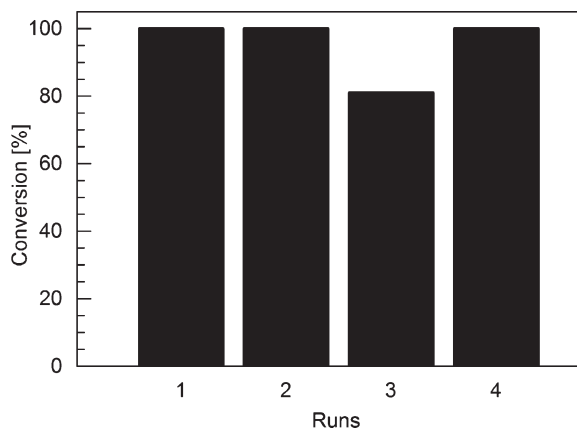


Fig. 11 Reuse of the CAPS-CuO catalyst in the oxidation of benzyl alcohol with intermediate thermal re-activation at 300 °C for 45 min. Reaction conditions: benzyl alcohol (1 mmol), anisole (0.1 mmol), toluene (3 mL), catalyst (60 mg), 24 h, 100 °C, atmospheric air.

## 4. Conclusions

Two types of copper oxide nanoparticles (CAPS-CuO and MES-CuO) were synthesized using the different buffers CAPS and MES, respectively, thoroughly characterized by imaging spectroscopy and diffraction techniques, and tested for the oxidation of benzyl alcohol to benzaldehyde with air at atmospheric pressure. Synthesis with the two buffers had a significant effect on the catalytic performance of the copper nanoparticles, and CAPS-CuO (CAPS buffer) gave better product yields than MES-CuO (MES buffer). HR-TEM characterization of the catalysts revealed a difference in exposed crystal facets with CAPS-CuO exposing mainly stable [001] facets possibly limiting its degradation during reaction. In addition, Rietveld refinements of XRD data showed a clear difference in CuO reduction between the catalysts, which likely influenced their catalytic performance.

The versatility of the oxidation reaction with CAPS-CuO was demonstrated by transforming benzylic, alicyclic and unsaturated alcohols to the desired products with exceptional selectivity ( $>99\%$ ). A significant increase in conversion was observed with benzyl alcohols containing electron donating groups (*p*-OCH<sub>3</sub> and *p*-CH<sub>3</sub>) compared to those containing electron withdrawing groups (*p*-Cl and *p*-CF<sub>3</sub>), suggesting a linear free energy relationship between activity and  $\sigma^+$ . Results from competitive oxidation of benzyl alcohols support that  $\alpha$ -C-H dissociation results in the formation of a stable benzylic carbocation intermediate. Moreover, the activity towards alicyclic alcohols was shown to follow the ring tension leaving larger rings more reactive. Importantly, CAPS-CuO was further found to be stable and reusable if thermally regenerated. Further studies, including kinetic isotopic studies and Hammett correlations, are in progress to elucidate the reaction mechanism in more detail.

The use of CuO as an efficient, inexpensive and selective heterogeneous catalyst for the oxidative dehydrogenation of alcohols proposes a new sustainable reaction protocol for carbonyl compound synthesis.

## Acknowledgements

Financial support from the UNIK research initiative Catalysis for Sustainable Energy and Lundbeck (R45-A3878) for the PhD study of R.P and C.E. is acknowledged. Authors would like to express their gratitude to Jonas Andersen for work on Rietveld refinements and Dr. Leonhard Schill for assistance with XPS acquisition.

## References

- 1 G. Tojo and M. Fernandez, in *Oxidation of Alcohols to Aldehydes and Ketones: A Guide to Current Common Practice*, Springer, New York, 2006.
- 2 (a) M. A. Halcrow, P. F. Knowles and S. E. V. Phillips, in *Handbook on Metalloproteins*, ed. I. Bertini, A. Sigel and H. Sigel, Marcel Dekker Inc, New York, 2001, p. 709; (b) Q. Jr. Lawrence and B. T. William, *Nature*, 2008, 455, 333.

- 3 (a) S. S. Shannon, *Science*, 2005, **309**, 1824; (b) J. Muzart, *Tetrahedron*, 2003, **59**, 5789; (c) J. Muzart, *Chem. – Asian J.*, 2006, **1**, 508; (d) T. F. Blackburn and J. Schwartz, *J. Chem. Soc., Chem. Commun.*, 1977, 157; (e) C. Liu, S. Tang and A. Lei, *Chem. Commun.*, 2013, **49**, 1324.
- 4 G. Cainelli and G. Cardillo, in *Chromium Oxidations in Organic Chemistry*, Springer, Berlin, 1984.
- 5 S. Zhang, L. Xu and M. L. Trudell, *Synthesis*, 2005, **11**, 1757.
- 6 G. B. Shul'Pin, Y. N. Kozlov, L. S. Shul'Pina, T. V. Strelkova and D. Mandelli, *Catal. Lett.*, 2010, **138**, 193.
- 7 R. A. Sheldon and J. K. Kochi, in *Metal-Catalysed Oxidations of Organic Compounds*, Academic Press, New York, 1981.
- 8 T. Mallat and A. Baiker, *Chem. Rev.*, 2004, **104**, 3037.
- 9 D. L. Pradeep, R. W. Smita, G. Harsh and P. P. Hankare, *J. Korean Chem. Soc.*, 2012, **56**, 539.
- 10 J. Mielby, R. Poreddy, C. Engelbrekt and S. Kegnæs, *Chin. J. Catal.*, 2014, **35**, 670.
- 11 Z. Junjiang, L. F. Joaquim, L. F. Jose and T. Arne, *Chem. – Eur. J.*, 2011, **17**, 7112.
- 12 S. J. Tauster, S. C. Fung, R. T. K. Baker and J. A. Horsley, *Science*, 1981, **211**, 1121.
- 13 C. Parmeggiani and F. Cardona, *Green Chem.*, 2012, **14**, 547.
- 14 G. C. Bond, P. A. Sermon, G. Webb, D. A. Buchanan and P. B. Well, *J. Chem. Soc., Chem. Commun.*, 1973, 444.
- 15 G. J. Hutchings, *J. Catal.*, 1985, **96**, 292.
- 16 M. Haruta, N. Yamada, T. Kobayashi and S. Ijima, *J. Catal.*, 1989, **115**, 301.
- 17 L. Prati and M. Rossi, *J. Catal.*, 1998, **176**, 552.
- 18 Z. Hou, N. Theyssen, A. Brinkmann, K. V. Klementiev, W. Grünert, M. Bühl, W. Schmidt, B. Spliethoff, B. Tesche, C. Weidenthaler and W. Leitner, *J. Catal.*, 2008, **258**, 315.
- 19 A. S. K. Hashmi, *Chem. Rev.*, 2007, **107**, 3180.
- 20 Guideline on the specification limits for residues of metal catalysts from the European Agency for the Evaluation of Medicinal Products (EMA), 2007 (<http://www.emea.europa.eu>). According to the guideline, only iron residues are considered entirely unproblematic. The limit for the total amount of platinoid-group metals is 5 mg kg<sup>-1</sup> (for dosages of up to 10 g per day). Compliance to this limit is usually assured by post-reaction scavenging/purification.
- 21 (a) C. E. Garrett and K. Prasad, *Adv. Synth. Catal.*, 2004, **346**, 889; (b) C. J. Welch, W. J. Albaneze, W. R. Leonard, M. Biba, J. DaSilva, D. Henderson, B. Laing, D. J. Mathre, S. Spencer, X. Bu and T. Wang, *Org. Process Res. Dev.*, 2005, **9**, 198; (c) J. T. Bien, G. C. Lane and M. R. Oberholzer, *Top. Organomet. Chem.*, 2004, **6**, 263.
- 22 H. Wang, F. Weibin, H. Yue, W. Jianguo, N. K. Junko and T. Takshi, *J. Catal.*, 2013, **299**, 10.
- 23 (a) S. Enthaler, K. Junge and M. Beller, *Angew. Chem., Int. Ed.*, 2008, **47**, 3317; (b) E. Nakamura and K. Sato, *Nat. Mater.*, 2011, **10**, 158.
- 24 R. Poreddy, E. J. Garcia-Suarez, A. Riisager and S. Kegnæs, *Dalton Trans.*, 2014, **43**, 4255.
- 25 (a) A. Alexakis, J. E. Backvall, N. Krause, O. Pamies and M. Dieguez, *Chem. Rev.*, 2008, **108**, 2796; (b) L. M. Stanley and M. P. Sibi, *Chem. Rev.*, 2008, **108**, 2887; (c) M. Meldal and C. W. Tornøe, *Chem. Rev.*, 2008, **108**, 295; (d) F. Collet, C. Lescot and P. Dauban, *Chem. Soc. Rev.*, 2011, **40**, 1926.
- 26 (a) D. Yu and Y. G. Zhang, *Proc. Natl. Acad. Sci. U. S. A.*, 2010, **107**, 20184; (b) D. Yu and Y. G. Zhang, *Adv. Synth. Catal.*, 2011, **353**, 163; (c) Y. G. Zhang, L. W. Chen and T. Lu, *Adv. Synth. Catal.*, 2011, **353**, 1055; (d) A. Martínez-Asencio, D. J. Ramon and M. Yus, *Tetrahedron*, 2011, **67**, 3140.
- 27 (a) C. Bolm, J. Legros, J. Le Pailh and L. Zani, *Chem. Rev.*, 2004, **104**, 6217; (b) B. D. Sherry and A. Fuerstner, *Acc. Chem. Res.*, 2008, **41**, 1500; (c) A. Correa, M. O. Garcia and C. Bolm, *Chem. Soc. Rev.*, 2008, **37**, 1108; (d) R. H. Morris, *Chem. Soc. Rev.*, 2009, **38**, 2282; (e) C. L. Sun, B. J. Li and Z. J. Shi, *Chem. Rev.*, 2011, **111**, 1293; (f) M. O. Garcia, *Angew. Chem., Int. Ed.*, 2011, **50**, 2216; (g) A. C. Gonzalez, K. Yoshida, R. Luque and P. L. Gai, *Green Chem.*, 2010, **12**, 1281.
- 28 O. David, M. B. Alina, A. R. Antonia, G. Walter, L. Rafael and K. C. Oliver, *Green Chem.*, 2013, **15**, 1530.
- 29 K. Qiang and Z. Yugen, *Green Chem.*, 2012, **14**, 1016.
- 30 I. E. Marko, M. Tsukazaki, P. R. Giles, S. M. Brown and C. J. Urch, *Angew. Chem., Int. Ed. Engl.*, 1997, **36**, 2208.
- 31 F. Zaccheria, N. Ravasio, R. Psaro and A. Fusi, *Chem. – Eur. J.*, 2006, **12**, 6426.
- 32 D. P. Cristina, F. Ermelinda and R. Michele, *J. Catal.*, 2008, **260**, 384.
- 33 R. M. Rioux and M. A. Vannice, *J. Catal.*, 2005, **233**, 147.
- 34 E. Christian, M. Philip, A. Jonas, Z. Lijuan, S. Kenny, L. Bin, H. Jun and Z. Jingdong, *J. Nanopart. Res.*, 2014, **16**, 2562.
- 35 Z. Zhongping, S. Haiping, S. Xiaoqiong, L. Dongfei, Y. Haidong and H. Mingyong, *Adv. Mater.*, 2005, **17**(1), 42.
- 36 Y. Li-Xia, J. Z. Ying, T. Hau, L. Liang and Z. Ling, *Mater. Chem. Phys.*, 2008, **112**, 442.
- 37 L. Jinping, H. Xintang, L. Yuanyuan, K. M. Sulieman, H. Xiang and S. Fenglou, *Cryst. Growth Des.*, 2006, **6**, 1690.
- 38 L. Jing, J. Jun, D. Zhao, Z. H. Shao, Y. H. Zhi, W. Li, W. Chao, H. C. Li, L. Yu, T. G. Van and L. S. Bao, *J. Colloid Interface Sci.*, 2012, **384**, 1.
- 39 J. F. Xu, W. Ji, Z. X. Shen, S. H. Tang, X. R. Ye, D. Z. Jia and X. Q. Xin, *J. Solid State Chem.*, 1999, **147**, 516.
- 40 A. B. Pereda, L. T. U. De, G. N. J. Illan, L. A. Bueno and V. J. R. Gonzales, *Appl. Catal., B*, 2014, **147**, 420.
- 41 N. S. McIntyre and M. G. Cook, *Anal. Chem.*, 1975, **47**, 2208.
- 42 <http://www.lasurface.com>, accessed on 13th May 2014.
- 43 P. Juyun, L. Kyounga, D. R. Rex and C. K. Yong, *Bull. Korean Chem. Soc.*, 2011, **32**, 3395.
- 44 M. Shimokawabe, H. Asakawa and N. Takezawa, *Appl. Catal.*, 1990, **59**, 45.
- 45 W. P. Dow, Y. P. Wang and T. J. Huang, *J. Catal.*, 1996, **160**, 155.
- 46 C. J. G. Van der Grift, A. Mulder and J. W. Geus, *Appl. Catal.*, 1990, **60**, 181.
- 47 S. D. Robertson, B. D. McNicol, J. H. Debaos, S. C. Kloet and J. W. Jenkins, *J. Catal.*, 1975, **37**, 424.
- 48 K. I. Shimizu, S. Kenji, S. Kyoichi and S. Atsushi, *Chem. – Eur. J.*, 2009, **15**, 2341.
- 49 (a) A. Abad, A. Corma and H. Garcia, *Chem. – Eur. J.*, 2008, **14**, 212; (b) P. Fristrup, L. B. Johansen and C. H. Christensen, *Catal. Lett.*, 2008, **120**, 184.